Postcombustion Measures for Cleaner Solid Fuels Combustion: Activated Carbons for Toxic Pollutants Removal from Flue Gases

G. Skodras,*[,†,‡,§] Ir. Diamantopoulou,[†] P. Natas,[†] A. Palladas,[†] and G. P. Sakellaropoulos[†,‡]

Chemical Process Engineering Laboratory, Department of Chemical Engineering, Aristotle University of Thessaloniki, Thessaloniki, Greece, Laboratory of Energy and Environmental Processes, Chemical Process Engineering Research Institute, Thessaloniki, Greece, and Institute for Solid Fuels Technology and Applications, Ptolemais, Greece

Received April 19, 2005. Revised Manuscript Received July 31, 2005

In this work the efficiency of postcombustion measures (i.e., activated carbon utilization) to achieve cleaner solid fuels combustion was evaluated. Thus, two commercial activated carbons (Calgon F400 and RWE active coke) were tested for removing toxic polluting compounds (Hg, PCBs, PCDD/Fs) from the gas phase. The effects of the pore structure and surface chemistry of the activated carbons tested were investigated, along with the sorption temperature and sulfur addition in carbon matrix. Experiments were realized in a bench-scale adsorption unit and in a commercial solid fuels-fired hot water boiler. The results showed that both activated carbons tested are suitable for the removal of toxic compounds (i.e., Hg, PCBs, PCDD/Fs) from the gas phase. Due to differences in Hg adsorptive capacity and adsorption rate, which are attributed to the diversified pore structure and surface chemistry of the activated carbons, RWE active coke is, presumably, more suitable for continuous Hg removal (i.e., activated carbon injection), while Calgon F400 is more suitable for batch one (packed column). For both activated carbons, Hg adsorption capacity was reduced with temperature increase, while it was enhanced by the presence of sulfur. Oxygen surface functional groups seem to be involved in Hg° adsorption mechanism. Lactones are believed to act as potential active sites for mercury adsorption, while phenols may act as inhibitors. The removal of PCBs and PCDD/Fs from the gas phase seems not to be a problem for the activated carbons tested, regardless of their pore structure or surface chemistry.

1. Introduction

A large amount of harmful compounds, such as volatile metals and polychlorinated compounds, are emitted during solid fuels combustion and incineration. The intensive use of solid fossil fuels for electricity production, the increase in residues combustion, and the application of recycling processes further aggravates the situation. Among toxic air pollutants, mercury, PCBs, and PCDD/Fs have drawn special attention due to their high toxicity and the consequent adverse effects on human health.[1] Their high level of bioaccumulation in the environment, and particularly in the food chain, justifies the very low legislative limits established (i.e., 0.1 ng/Nm^3 and 50 μg/Nm^3 for PCDD/F and Hg, respectively) and the increased concern for reduced emissions. Coal-fired power plants and waste incinerators have been recognized as major emission sources due to the high mercury content and the presence of chlorine in the utilized fuels.[2,3] Under the combustion zone conditions, mercury is completely volatilized and, in the complex environment of the flue gases duct, is partly transformed to its oxidized form (probably $HgCl_2$ and in some cases HgO), with the elemental mercury being the predominant form.[4] The control of mercury emissions strongly depends on the mercury speciation, since it is more difficult to capture Hg° than its oxidized forms.[5] Conventional pollution abatement technologies were proven inefficient in controlling gas-phase mercury emissions, due to its insolubility in water, chemical inertia, and high volatility.[5] However, materials such as activated carbons, calcium-based sorbents, fly ashes,

* Author to whom correspondence should be addressed. Tel: +30-2310-996225. Fax: +30-2310-996168. E-mail: skodras@vergina.eng.auth.gr.

† Aristotle University of Thessaloniki.

‡ Chemical Process Engineering Research Institute.

§ Institute for Solid Fuels Technology and Applications.

(1) *Toxicological Effects of Methylmercury*; Committee on the Toxicological Effects of Methylmercury, National Research Council; National Academy Press: Washington, DC, 2000.

(2) Thomas, M. K.; Gaurtin, M.; Fuertes B. A. *Abatement of Environmentally Unfriendly Species in Combustion and Gasification System*; Technical Report No. 5, Contract No. ECSC 7220-PR113, Northern Carbon Research Laboratories-University of Newcastle, Centre D'etudes et de Recherchers du Charbon, Instituto National del Carbon, 2002.

(3) Keating, M. H.; Mahaffey, K. R.; Schoeny, R.; Rice, G. E.; Bullock, O. R.; Ambrose, R. B., Jr.; Swartout, J.; Nickols, J. W. *Mercury Study Report to Congress*; EPA-452/R-97-003; U.S. Environmental Protection Agency, Office of Air Quality Planning and Standards and Office of Research and Development, U.S. Environmental Protection Agency: Research Triangle Park, NC, 1997; Vols. I−VIII.

(4) Senior, C.; Sarofim, A.; Zeng, T.; Helble, J.; Mamani-Paco, R. *Fuel Process. Technol.* **2000**, *63*, 197−213.

(5) Chang, R.; Offen, G. R. *Power Eng.* **1995**, *99*, 51−57.

10.1021/ef050112h CCC: $30.25
Published on Web 10/07/2005

and zeolites could be effectively used for mercury removal from flue gases.

Activated carbons are considered as "general purpose" materials, and their extended surface area and high surface reactivity renders them suitable for Hg° adsorption.[6,7] Several investigations have been conducted to evaluate their behavior.[2,9−13] Generally, it was found that the structural properties and the surface chemistry affect the mercury adsorption ability of the activated carbons.[8,12,14] However, Hg° adsorption mechanisms are not clarified, and efforts to correlate that with structural and chemical characteristics of activated carbons were not completely successful. Vidic et al.[8] found that a proper pore size distribution permitting the entrance of mercury into the pores and a large surface area offering a high number of active sites are necessary for increased mercury uptake. Thus, activated carbons with a large BET surface area and high percentage of micropores exhibited enhanced efficiency in mercury removal[9,15] and increased equilibrium adsorptive capacity.[10] The effect of particle size on Hg° adsorption was also investigated,[9,12] and the results showed that small particle size enhances mercury sorption, due to reduced intraparticle mass transport limitations. Previous studies have shown that sulfur impregnated activated carbons exhibit significantly enhanced mercury adsorptive capacity.[2,16−19] The sulfur impregnation temperature and consequently the sulfur allotropes were found to be the most important parameters defining the efficiency of these sorbents.[17−20] The effect of adsorption temperature was also studied, and it was found that, regardless of the activated carbon used, mercury uptake by virgin or sulfur impregnated carbons decreases with temperature increase.[21−23]

The surface chemistry of the activated carbons also influences Hg° adsorptive capacity and affects their interaction with the adsorbate.[24−28] The properties of the parent carbonaceous material and the preparation conditions are important factors affecting the presence of acidic and basic groups that determine surface chemistry.[24,25] Thus, low-temperature oxidation (200−400 °C) results in the more acidic L-type carbons, while high-temperature activation (i.e., 1000 °C), either in pure CO_2 or under vacuum, gives H-type carbons of basic character.[24,26] Surface oxygen-containing groups such as carbonyl, carboxyl, phenolic hydroxyl, lactone, and quinone groups are representative acidic groups, while other surface oxides (i.e., chromenes, ethers, and carbonyls) are associated with the basic behavior. Furthermore, pyrone-like structure and the π-electrons of the graphene layers that could act as Lewis bases and nitrogen-containing groups contribute to the basic character.[26,27] Generally, it is considered that surface oxygen complexes provide active sites for Hg° attachment.[14,29] Surface groups are determined by wet (Boehm, potentiometric titration) or dry (FTIR, XPS, TPD) techniques. Concerning acidic groups, Boehm titration provides information limited to phenols, lactones, and carboxylic acids, neglecting all other groups.[30−32] Quantification of them is based on the assumption that $NaHCO_3$ neutralizes only carboxylic, Na_2CO_3 carboxylic, and lactonic groups, while NaOH neutralizes carboxylic, lactonic, and phenolic ones. Thus, carboxylic, lactonic, and phenolic oxygen-containing groups can be calculated. However, since Boehm titration accounts only for 50% of the total oxygen content, it is useful, mainly, when used in combination with other techniques.[28] TPD can assess all functional groups qualitatively, and when coupled with MS quantitative information for the functional groups that decompose below 1250 °C can be obtained.[33] Carboxylic acids and lactone groups evolve CO_2 upon heating, and carboxylic anhydride produces both CO and CO_2. CO derives from phenols, ethers, and carbonyls/quinines groups.[34]

Limited research has been done to study the PCB and/or PCDD/F adsorption on activated carbons from flue gases or liquid phase, although quite encouraging results were recently obtained.[23,35,36] According to Brasseur et al.,[37] carbon-based sorbents, tested in a bench-scale rig, exhibited the best adsorption performance of

(6) Jurng, J.; Lee, T.; Lee, G.; Lee, S.; Kim, B.; Seier, J. *Chemosphere* **2002**, *47*, 907−913.
(7) Anton Lopez, A. M.; Tascon, M. D. J.; Martinez-Tarazona, M. R. *Fuel Process. Technol.* **2002**, *77*−*78*, 353−358.
(8) Vidic, D. R.; Liu, W.; Brown, D. T. *Development of Novel Activated Carbon-Based Adsorbents for Control of Mercury Emissions from Coal-Fired Power Plants*; Final Report No. DE-FG22-96PC96212, U.S. Department of Energy, Federal Energy Technology Center, University of Pittsburgh, 2001.
(9) Krishman, S. V.; Gullett, B. K.; Jozewicz, W. *Environ. Sci. Technol.* **1994**, *28*, 1506−1512.
(10) Huang, H. S.; Wu, J. M.; Livengood, C. D. *Hazard. Waste Hazard. Mater.* **1996**, *13*, 107−120.
(11) Korpiel, J. A.; Vidic, R. D. *Environ. Sci. Technol.* **1997**, *31*, 2319−2325.
(12) Carey, T. R.; Hargrove, O. W., Jr.; Richardson, C. F.; Chang, R.; Meserole, F. B. J. *J. Air Waste Manage. Assoc.* **1998**, *48*, 1166−1174.
(13) Rostam-Arabi, M.; Chen, S. G.; His, H.-C.; Rood, M.; Chang, R.; Carey, T.; Hargrove, B.; Richardson, C.; Rosenhoover, W.; Meserole, W.; Meserole, F. *Novel Vapour Phase Mercury Sorbents*; Proceedings of the First EPRI-DOE-EPA Combined Utility Air Pollutant Control Symposium, Session B, Washington, DC, Aug 25−29, 1997.
(14) Li, Y. H.; Lee, C. W.; Gullett, B. K. *Carbon* **2002**, *40*, 65−72.
(15) Serre, S. D.; Silcox, G. D. *Ind. Eng. Chem. Res.* **2000**, *39*, 1723−1730.
(16) His, H.; Rood, M.; Rostam-Abadi, M.; Chen, S.; Chang, R. *Environ. Sci. Technol.* **2001**, *35*, 2785−2791.
(17) Lee, S.; Park, Y. *Fuel Process. Technol.* **2003**, *84*, 197−206.
(18) Vitolo, S.; Seggiani, M. *Geothermics* **2002**, *31*, 431−442.
(19) Liu, W.; Vidic, R.; Brown, T. D. *Environ. Sci. Technol.* **1998**, *32*, 531−538.
(20) Skodras, G.; Orfanoudaki, T.; Kakaras, E.; Sakellaropoulos, G. P. *Fuel Process. Technol.* **2002**, *77*−*78*, 75−87.
(21) Vidic, R.; Chang, M.; Thurnau, R. *J. Air Waste Manage. Assoc.* **1998**, *48*, 247−255.
(22) Karatza, D.; Lancia, A.; Musmarra, D.; Zucchini, C. *Exp. Therm. Fluid Sci.* **2000**, *21*, 150−155.
(23) Sotelo, L. J.; Ovejero, G.; Delgado, A. J.; Martinez, I. *Water Res.* **2002**, *36*, 599−608.
(24) Laszlo, K. J.; Tombacz, E. *Anal. Sci.* **2001**, 1741−1744.
(25) Mattson, S. J.; Mark, B. H. *Activated Carbon. Surface Chemistry and Adsorption from Solution*; Marcel Dekker: New York, 1971; pp 29−46.
(26) Lahaye, J. *Fuel* **1997**, *77*, 543−547.
(27) Bansal, C. R.; Donnet, B. J.; Stoeckli, F. *Active Carbon*; Marcel Dekker: New York and Basel, 1988; pp 28−50.
(28) Figueiredo, L. J.; Pereira, R. F. M.; Freitas, A. M. M.; Orfao, M. J. J. *Carbon* **1999**, *37*, 1379−1389.
(29) Li, H. Y.; Lee, W. C.; Gullett, K. B. *Fuel* **2003**, *82*, 451−457.
(30) Salame, I. I.; Bandosz, T. J. *J. Colloid Interface Sci.* **2001**, *240*, 252−258.
(31) Contescu, A.; Contescu, C.; Putyera, K.; Schwarz, J. A. *Carbon* **1997**, *35*, 83−94.
(32) Boehm, H. P. *Carbon* **2002**, *40*, 145−149.
(33) Castilla Moreno, C.; Marin Carrasco, F.; Mueden, A. *Carbon* **1997**, *35*, 1619−1626.
(34) Mirasol-Rodriguez, J.; Cordero, T.; Vivo, G.; Piriz, J.; Tancredi, N.; Rodriguez, J. J. *Ind. Eng. Chem. Res.* **2002**, *41*, 6042−6048.
(35) Mastral, M. A.; Garcia, T.; Murillo, R.; Callen, S. M.; Lopez, M. J.; Navarro, V. M. *Ind. Eng. Chem. Res.* **2003**, *42*, 5280−5286.
(36) Everaert, K.; Baeyens, J.; Degreve, J. *Environ. Sci. Technol.* **2003**, *37*, 1219−1224.
(37) Brasseur, A.; Gambin, A.; Laudet, A.; Marien, J.; Pirard, J.-P. *Chemosphere* **2004**, *56*, 745−756.

chlorinated organic compounds. Results obtained by Everaert and Baeyens[38] illustrated the excellent overall efficiency of activated carbons in removing PCDD/Fs from the flue gases in a municipal solid waste incinerator. This behavior was also noticed by McKay,[39] who reviewed PCDD/Fs characterization, formation, and minimization during MSW incineration. Similarly to mercury adsorption, activated carbons with increased porosity showed enhanced efficiency in organic compound (PAH) removal from the gas phase.[23,35−38] The existence of large mesopores and the percentage of micropores seem to be important factors and greatly affect the adsorption process.[35,37]

In the case of pilot or full-scale tests, the EPA 60,[40] the EPA 101A, and cold vapor atomic absorption spectroscopy are generally used for mercury sampling, measurement, and speciation.[41−44] Laudal et al.[45] employed a modification of the EPA 29 method, the Ontario Hydro (OH) method for measuring total and speciated mercury. Sampling and analysis of PCDD/Fs are usually realized according to the EPA 23A[46] or VDI 3499[47] standard methods.

In this work, the efficiency of two commercial activated carbons (Calgon F400 and RWE active coke) in removing toxic polluting compounds (Hg, PCBs, PCDD/Fs) from the gas phase was evaluated. The effects of the pore structure and surface chemistry of the activated carbons tested were investigated, along with the sorption temperature and sulfur addition in carbon matrix. Experiments were realized in a bench-scale adsorption unit and in a commercial solid fuels-fired hot water boiler.

2. Methodology

2.1. Samples Preparation. The efficiency of two commercially available activated carbons, Calgon F400 and RWE active coke, in removing toxic polluting compounds from the gas phase was evaluated. Prior to use, samples were outgassed overnight under vacuum. Sulfur addition in the activated carbons was accomplished by high heating with high purity sulfur flakes[17,19,20] as described in detail elsewhere.[20] Briefly, preweighted amounts of activated carbon and sulfur were heated under nitrogen flow for 2 h at 600 °C. At these conditions a homogeneous sulfur distribution in the pores is achieved,[20] and the sulfur is primarily found in the form of short S_2−S_6 chains with more reactive terminal atoms that penetrate the carbon structure without blocking the micropores.[16,19]

2.2. Characterization of Samples. Physical adsorption methods (i.e., N_2 and CO_2 adsorption) were employed for pore structure characterization. A conventional volumetric apparatus (Quantasorb multiple sample manifold) was used for the N_2 adsorption experiments, and the dynamic method was elaborated to obtain adsorption isotherms at low temperature (77 K). CO_2 adsorption isotherms were obtained by using a laboratory volumetric apparatus, and the static method at room temperature was used. Prior to N_2 and/or CO_2 adsorption measurements, samples where degassed overnight at 110 °C under vacuum. BET multiple point[48] and Dubinin−Raduchevich[49] equations were used to calculate surface areas from N_2 and CO_2 adsorption, respectively. Molecular cross-sectional areas were considered 0.253 nm^2 for CO_2 at 298 K and 0.162 nm^2 for N_2 at 77 K.[50] The pore size distribution of the activated carbons was calculated by using Medek[51] and Horvath−Kawazoe[52] methods for the micropores, while Kelvin[48] method was used for the mesopores.

Oxygen functional groups, present in both activated carbons, were measured by using basic−acid titration based on the Boehm method[53] and TPD−MS measurements. According to the Boehm method, 1 g of each sample was suspended and shaken for 24 h in 50 mL of 0.05 N solutions of $NaHCO_3$, Na_2CO_3, NaOH, and HCL in sealed quartz flasks. The obtained slurry was filtered, and the excess base or acid of the filtrate was titrated with HCl for basic[33] or NaOH for acid groups, respectively. The pH of the surface of both activated carbons was measured also. Thus, 0.4 g of dry sample was suspended in 20 mL of distilled water and stirred for 24 h in a sealed vial. The slurry was filtered, and the pH of the filtrate was measured.

Since acid−basic titration accounts only for 50% of the total oxygen content, the temperature programmed desorption (TPD) technique was also employed. TPD analyses were conducted by using a ThermoFinnigan TPD/R/O 1100 equipped with a TCD and coupled with a quadrupole mass spectrometer (Balzer, Benchtop Gas Analyzer OMNISTAR). Predried samples (100 mg) were placed in a quartz tube reactor and heated under He flow (55 cm^3/min) and 10 °C/min heating rate. The PeakFit software that is based on the methodology developed by Figueiredo et al.[28] was used to fit the TPD curves with Gaussian peaks. The evolved gases (i.e., CO, CO_2) were continuously monitored.

A ThermoFinnigan Flash EA 1112 CHNS elemental analyzer was used to obtain the ultimate analysis of the activated carbons, pure or sulfur impregnated.

2.3. Bench-Scale Tests. A schematic representation of the PCB and Hg adsorption unit is shown in Figure 1. Two analogous units were constructed and used, one for PCB adsorption tests and one for mercury adsorption tests. PCB powder was placed in a homemade permeation device, which had the ability when heated to release the PCB in the gas phase at constant concentration. A mercury permeation tube was procured from VICI Valco Instruments as a mercury source. The permeation device was secured in a U-tube holder, and nitrogen at preadjusted constant flow passed through it. The U-tube was placed in a constant temperature chamber where the PCB temperature could be controlled between 40 and 60 °C, while the mercury temperature was controlled from

(38) Everaert, K.; Baeyens, J. *Waste Manage.* **2004**, *24*, 37−42.
(39) McKay, G. *Chem. Eng. J.* **2002**, *86*, 343−368.
(40) EPA 29. U.S. Environmental Protection Agency, Method 0060: Determination of Metals in Stack Emissions, Revision 0, December 1996, http://www.epa.gov/epaoswer/hazwaste/test/main.htm.
(41) EPA 101. Determination of Particulate and Gaseous Mercury Emissions from Chlor-Alkali Plants-Air Streams. Adopted March 28, 1986. http://www.epa.gov/epaoswer/hazwaste/test/main.htm.
(42) EPA 7471A. Mercury in solid or semisolid waste (Manual Cold-Vapour Atomic Absorption Spectroscopy). Revision September 1994, http://www.epa.gov/epaoswer/hazwaste/test/main.htm.
(43) Yousif, S.; Siemens, V.; Pintus, N.; Boavida, D. Technical Progress Report No. 2, Contract No. 7220/PR-088, 2001.
(44) Stuart, J. Development of an experimental system to study mercury uptake by activated carbons under simulated flue gas conditions, Ph.D. Thesis, University of Pittsburgh, Pittsburgh, PA, 2002.
(45) Laudal, D.; Brown, T.; Nott, B. *Fuel Process. Technol.* **2000**, *65−66*, 157−165.
(46) *Method 0023A: Sampling Method for Polychlorinated Dibenzo-p-Dioxins and Polychlorinated Dibenzofuran Emissions from Stationary Sources*, revision 1; U.S. Environmental Protection Agency: Research Triangle Park, NC, December 1996.
(47) VDI Verein Deutscher Inginieure Method 3499. Emission measurement − Determination of polychlorinated dibenzo-*p*-dioxins (PCDDs) and dibenzofurans (PCDFs) − Filter/condenser method; February 2004, www.vdi.de.
(48) Gregg, S. J.; Sing, K. J. W. *Adsorption Surface Area and Porosity*; Academic Press: London 1982; pp 41−105.
(49) Dubinin, M. M. *Carbon* **1989**, *27*, 7, 457−467.
(50) Walker, P. L., Jr.; Cariaso, O.; Patel, R. L. *Fuel* **1968**, *47*, 322.
(51) Medek, J. *Fuel* **1977**, *56*, 131−133.
(52) Horvath, G.; Kawazoe, K. *J. Chem. Eng. Jpn.* **1983**, *16*, 470−475.
(53) Boehm, H. P. *Adv. Catal.* **1966**, *16*, 179.

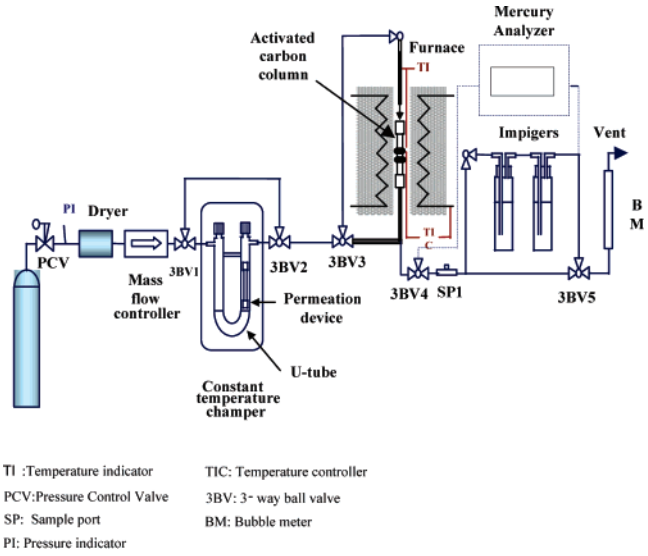

Figure 1. Schematic diagram of mercury and PCB adsorption test rig.

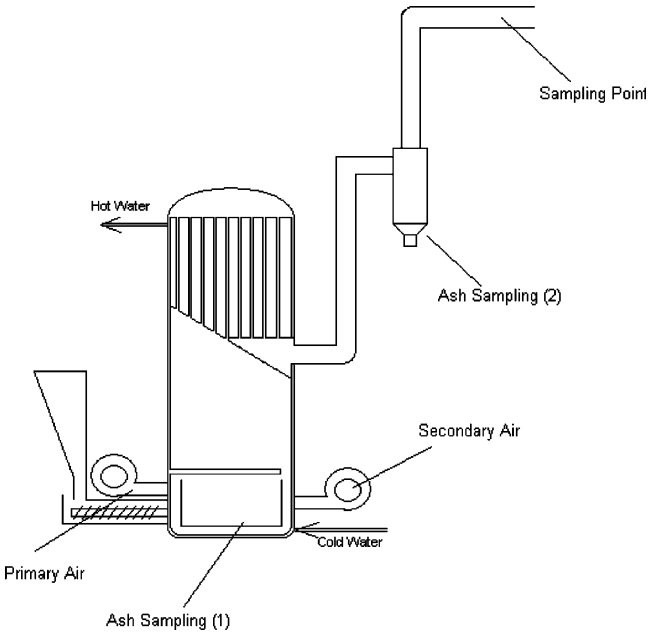

Figure 2. Schematic diagram of the hot water boiler.

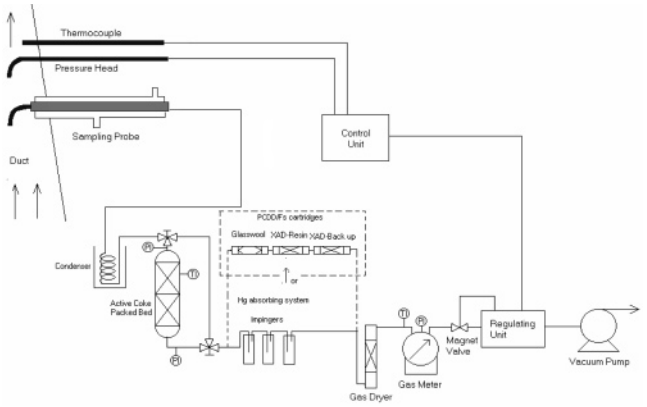

Figure 3. Schematic diagram of gas sampling from the hot water boiler and activated carbon testing.

Table 1. Ultimate Analysis of Raw and Sulfur Impregnated Activated Carbons

	activated carbon			
compound	RWE	(S)RWE	F400	(S)F400
C	89.09	84.59	86.8	80.9
H	0.23	0.10	0.34	0.11
N	0.37	0.21	0.53	0.54
S	0.76	4.37	0.96	7.16
O*	0.05	1.32	4.00	3.9
Ash	9.50	9.41	7.37	7.39

60 to 100 °C. The outlet of the U-tube contains PCB or mercury in the gas phase, and the initial PCB-52 (2,5,2′, 5′-tetrachlorobiphenyl) concentration was 0.15 ppb, while the Hg° inlet was kept constant at 0.35 ng/cm^3. For the adsorption experiments, this stream was fed in the heated activated carbon column that was enclosed in a temperature-controlled oven. The main body of the adsorption tests was conducted with activated carbon mass of 20 mg (particle size 150−250 μm), mixed with 1 g of sand, and the sorption temperature ranged from 50 to 200 °C. To account for the effects of carbon dosage and particle size, tests were performed also with 20−200 mg of activated carbon and activated carbon particles from 76 to 1000 μm. The concentration of the PCBs was measured in the gas phase before and after the activated carbon column by a Carlo-Erba MEGA 5360 gas chromatograph equipped with 63Ni electron capture detector. A DB-5 capillary column (J&W 15 m × 0.53 mm ID, film thickness 0.15 μm) was used. The concentration of elemental mercury in the gas stream was continuously monitored and recorded by a Mercury Instruments Analyzer (VM 3000 Mercury Vapour Monitor) based on cold vapor atomic adsorption spectroscopy.

2.4. Pilot-Scale Tests. Pilot-scale tests were performed in a commercial hot water boiler of 756 kW$_{th}$ (Figure 2) equipped with an automatic solid fuel burner. The combustion was controlled automatically by reducing or increasing the amount of air entering the chamber via a fan. The solid fuel entered the burner by means of a screw-type feeder. Primary air was distributed through a duct around the fuel, while secondary air was fed just above the fuel supply. The raw gases passed through a cluster of tubes, surrounded from the cooling water, before entering the duct. A multicyclone was used for flue gas dedusting. The combustion gases were removed by means of natural convection through an 8-m high chimney. Activated carbon was placed in a packed bed operating below 200 °C, since at higher temperatures the formation of PCDD/Fs was still taking place. The packed column consisted of a stainless steel tube, 1/2" OD and 24" length, and the mass of activated carbon was 2.5 g (150−250 μm) mixed with 125 g of quartz sand to increase the gas−solid contact time. A slip stream of 2 Nm^3, dry/hr was isokinetically sucked from the stack and passed through the activated carbon column for 5 h. PCDD/F and mercury measurements were performed before and after the activated carbon packed column to test its removal capacity. Schematic diagrams of the test units for sampling and PCDD/F and Hg° adsorption capacity measurements are given in Figure 3. Virgin and sulfur impregnated F400 and RWE activated carbons were tested for their ability to remove PCDD/F and Hg from the flue gases.

3. Results and Discussion

3.1. Characterization of Samples. The elemental analysis results of the activated carbons tested (both virgin and sulfur impregnated) are given in Table 1. Apart from oxygen concentration, both samples present similar elemental composition. The issue of oxygen presence and functional groups will be discussed in a later section.

The N_2 adsorption isotherms for the commercial activated carbons (RWE and F400) are given in Figure 4. Both isotherms are of type IV according to IUPAC

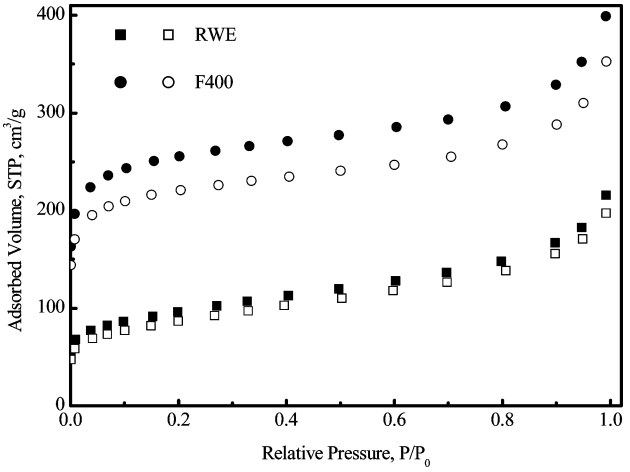

Figure 4. N_2 adsorption isotherms of the activated carbons tested (closed points: raw; open points: sulfur impregnated).

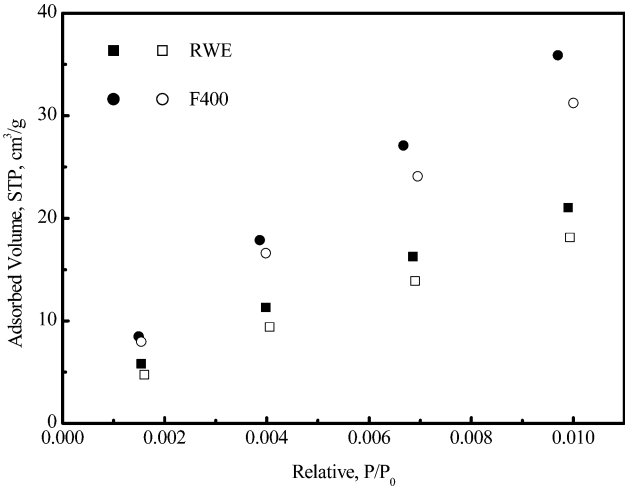

Figure 5. CO_2 adsorption isotherms of the activated carbons tested (closed points: raw; open points: sulfur impregnated).

classification; however, F400 exhibits much higher N_2 adsorption capacity, indicating a better developed pore structure. The CO_2 adsorption capacity of F400 is much higher than the one of RWE active coke (Figure 5), indicating a micropore structure for F400. This is further evident by the total and the micropore volume of the samples given in Table 2. Thus, in comparison to RWE, F440 has more than double BET and almost double CO_2 surface area. Despite the high impregnation temperature,[20] the addition of sulfur caused a limited, but noticeable, decrease in N_2 adsorptive capacity (Figure 4) for both activated carbons tested, due to possible pore blocking. Consequently, the BET surface area also decreases slightly (Table 2). Reflecting the above, an analogous small decrease in CO_2 adsorption capacity was observed (Figure 5).

The Medek pore size distribution curves of the F400 and RWE activated carbons are of similar shape (Figure 6). However, almost double values were obtained for F400 due to its micropore structure that is proclaimed by its increased CO_2 adsorption capacity. This is further reverberated on the Horvath−Kawazoe pore size distribution curves (Figure 7), which revealed a wider pore size distribution for RWE, since only ∼45% of the total pore volume corresponds to pore widths less than 5 nm. Thus, a clear shift to higher pore size is observed for the RWE active coke. Similarly, the Kelvin method revealed a narrow pore size distribution for F400 (Figure 8), while a much wider one was observed for RWE active coke, also accompanied by a peak between 30 and 50 Å. Due to the limited effect of sulfur addition on the N_2 and CO_2 adsorption capacities of the commercial active cokes, the micropore (Medek, Horvath−Kawazoe) and the mesopore (Kelvin) size distribution curves of the sulfur impregnated samples are almost identical with the ones obtained for the virgin materials (Figures 6−8). The average width of the micropore, L, evaluated by using a DR equation shows similar values (0.75−0.76 nm) for the carbons tested, suggesting the presence of similar micropore size distribution for both virgin and sulfur impregnated activated carbons.

Therefore, F400 possesses a well-developed micropore structure and consequently high micro- and total pore volume as well as BET surface area. RWE is a mesoporous material with lower pore volume and BET surface area. Sulfur addition has only slightly affected the initial pore structure of the activated carbons tested.

Figure 9 shows a comparison of the TPD plots obtained for the activated carbons tested. Up to 500 °C the TPD plots are quite similar, exhibiting a wide maximum that is more distinguishable for F400; however, significant differences are observed above this temperature. In the temperature region 500−700 °C, the TPD curve increases smoothly for F400, while a sharp peak with maximum at ∼650 °C is observed for RWE. Both activated carbons present a wider peak between 700 and 1000 °C, with maximum at ∼900 °C and a steep ascent above 1000 °C with maximum at ∼1090 °C. The TPD curves combine all the desorbed species during the thermal treatment (i.e., water, hydrogen, carbon monoxide, and carbon dioxide) at different temperatures. Thus, the complex TPD spectra obtained should be deconvoluted to estimate the surface composition. A multiple Gaussian function was elaborated for fitting the TPD procedure,[28] and the deconvoluted TPD profiles are given in Figures 10 and 11. The deconvolution resulted in 10 curves for F400 and nine for RWE, indicating the observed differences in the TPD spectra. When carbon materials are heated, the various surface oxygen functional groups (i.e., carbonyls, carboxyls, phenols, lactones, ethers, quinines, and anhydrides) decompose and release CO_2 and CO at different temperatures. However, the TPD peaks are not easily assigned to specific surface groups since the peaks could be affected by the structural properties of the activated carbon, the heating rate, or even the experimental apparatus.[28,54−56] Generally, the CO_2 released at low temperatures comes from acidic surface groups, while the CO, which is released at higher temperatures, comes from weak acidic and basic groups that are more thermally stable. Thus, CO_2 comes from carboxyls below 400 °C and/or from lactones at high temperatures, while CO is released above 600 °C from phenols, carbonyls, ethers, and quinines.[28,30] Carboxylic anhydrides produce

(54) Falconer, J. L.; Schwarz, J. A. *Catal. Rev.−Sci. Eng.* **1983**, *25*, 141−227.
(55) Boehm, H. P.; Bewer, G. In *Contribution to the development of reactor graphites and pyrocarbons: irradiation behaviour, model conceptions and characterization*, Papers presented at the 4th London International Carbon and Graphite Conference, London, Sept 23−27, 1974; Kernforschungsanlage Jülich: Jülich, Germany, 1974; p 344.
(56) Boehm, H. P. *Carbon* **1994**, *32*, 759−769.

Table 2. Pore Structure Characteristics and Hg° Adsorption Capacity of Raw and Sulfur Impregnated Activated Carbons

sample	BET (m^2/g)	CO_2 area (m^2/g)	total pore volume (cm^3/g)	micropore volume (% of total)	mean pore diameter (nm)	Hg adsorption capacity[a] (ng Hg/mg AC)
RWE	343	519	0.283	50.5	0.755	394
(S)RWE	310	486	0.265	47.8	0.763	655
F400	816	881	0.489	85.1	0.754	680
(S)F400	779	832	0.447	83.0	0.762	1158

[a] 20 mg AC, 50 °C, 360 min.

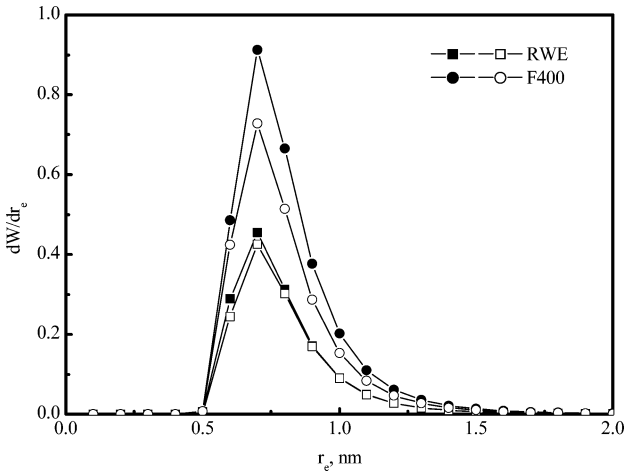

Figure 6. Medek pore size distribution curves of the activated carbons tested (closed points: raw; open points: sulfur impregnated).

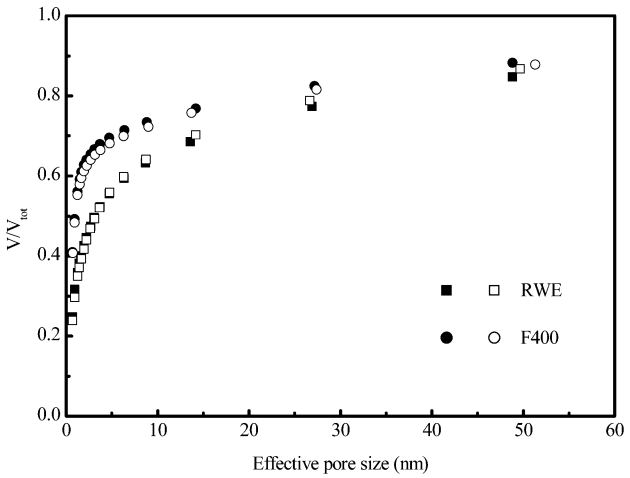

Figure 7. Horvath−Kawazoe pore size distribution curves of the activated carbons tested (closed points: raw; open points: sulfur impregnated).

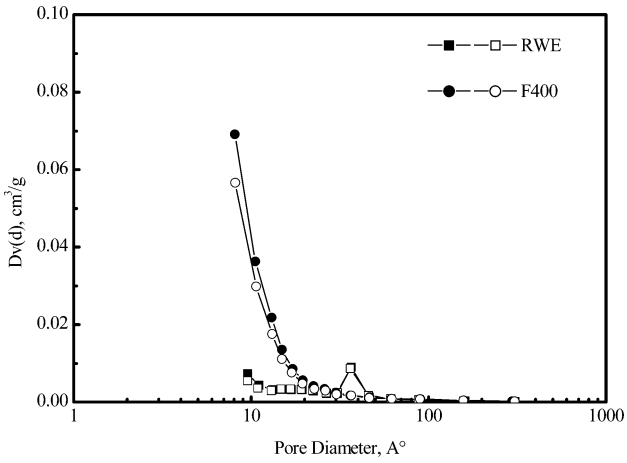

Figure 8. Kelvin pore size distribution curves of the activated carbons tested (closed points: raw; open points: sulfur impregnated).

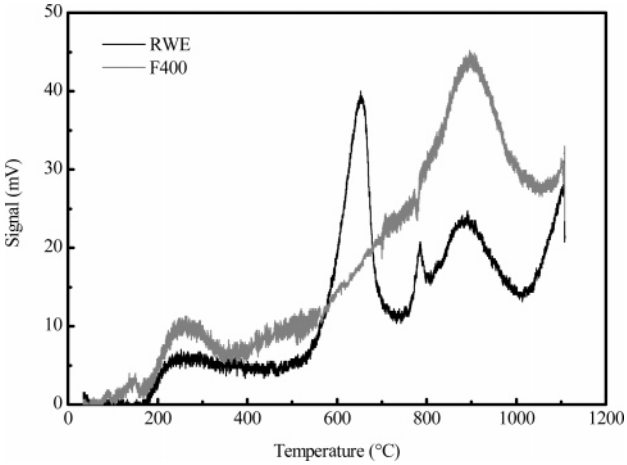

Figure 9. TPD profiles of the activated carbons tested.

both CO_2 and CO in the temperature region ~400−700 °C, and phenols, ethers, carbonyls, and quinines generate a CO peak between 700 and 1000 °C.[28,30]

The CO and CO_2 evolution curves, as obtained from the mass spectrometer during the TPD tests, are given in Figures 12 and 13 for RWE and F400, respectively. The evolution of CO_2 starts at 100−200 °C, while CO production begins above 400 °C. F400 yielded 50% more CO than RWE, while the latter released three times more CO_2 (Table 3). For both activated carbons tested, CO is more abundant than CO_2, indicating the presence of a much larger number of uni-oxygen surface groups. That is particularly true for F400, since the CO yield for this activated carbon is 7 times higher than that of CO_2. Gas evolution curves were deconvoluted[28] to account for the different surface oxygen functional groups, and the obtained results are given in Figures 14−17. The deconvoluted CO_2 curve for RWE presented five peaks (Figure 14, at 270, 454, 621, 662, and 719 °C), while in the corresponding one for F400 we found six peaks (Figure 15, at 139, 260, 365, 470, 586, and 672 °C). As mentioned previously, CO_2 is produced from the decomposition of carboxyls below 400 °C, lactones between 400 and 700 °C, and carboxylic anhydrides above 700 °C.[28] However, the phenomena are much more complex, since the temperature limits are only indicative, and depending on the structural properties of the activated carbon, the dissociation of carboxyls and lactones takes place, more or less, in parallel in the temperature region 200−700 °C.[28,54−56] The above are further discussed and elucidated in the following paragraphs, along with the Boehm titration results. For both

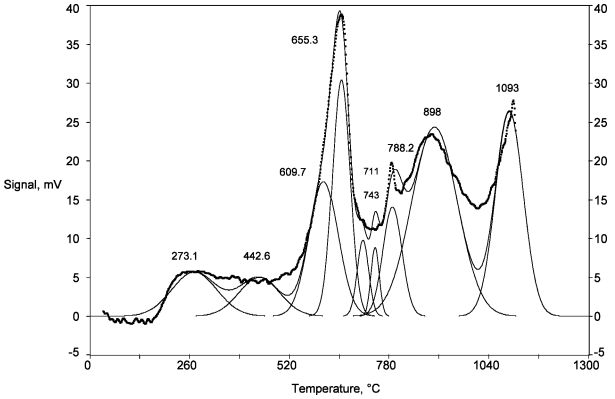

Figure 10. Deconvoluted TPD profile of the RWE activated carbon.

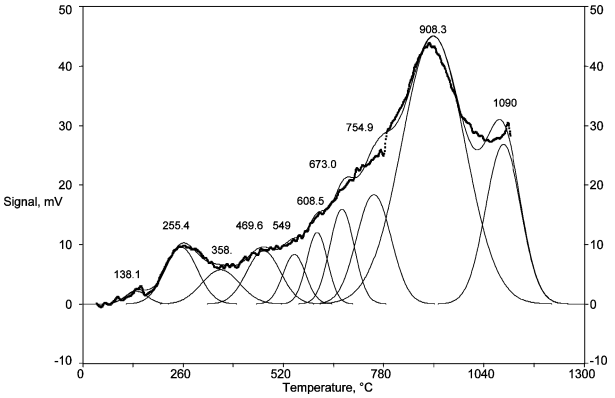

Figure 11. Deconvoluted TPD profile of the F400 activated carbon.

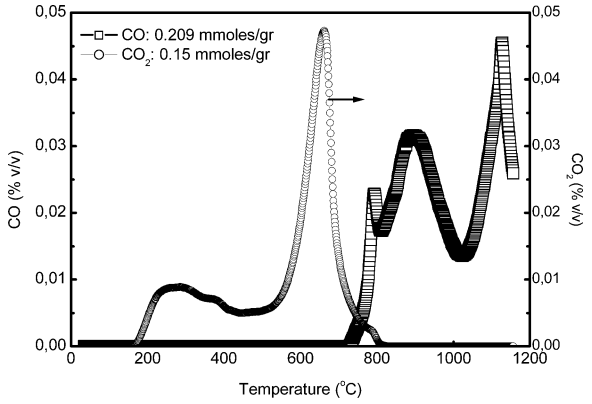

Figure 12. CO and CO_2 evolution curves of the RWE activated carbon during TPD testing.

activated carbons, four peaks were observed in the deconvoluted CO curves (Figures 16 and 17) that are attributed to the decomposition of carboxylic anhydrides and/or ethers (at 585 and 770 °C) and of ethers, carbonyls, and quinones between 700 to 1100 °C.

For both activated carbons tested, Boehm titration results, along with measured pH values and the different estimated oxygen surface functional groups, are given in Tables 4 and 5. The latter were calculated according to the assumption that $NaHCO_3$ neutralizes only carboxylic, Na_2CO_3 carboxylic, and lactonic groups, while NaOH neutralizes carboxylic, lactonic, and phenolic ones. The basic and acid character of an activated carbon can be approximately defined by its HCl and NaOH titration values, respectively. For both RWE and

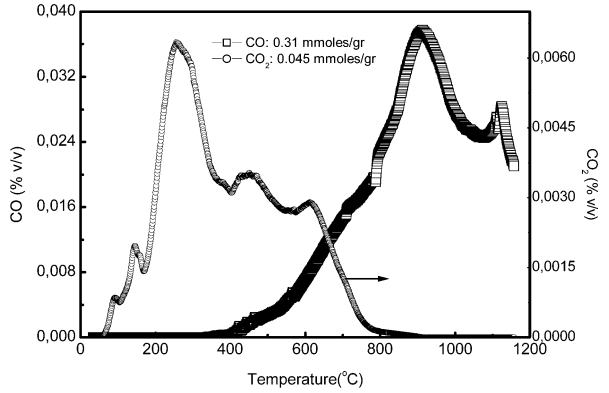

Figure 13. CO and CO_2 evolution curves of the F400 activated carbon during TPD testing.

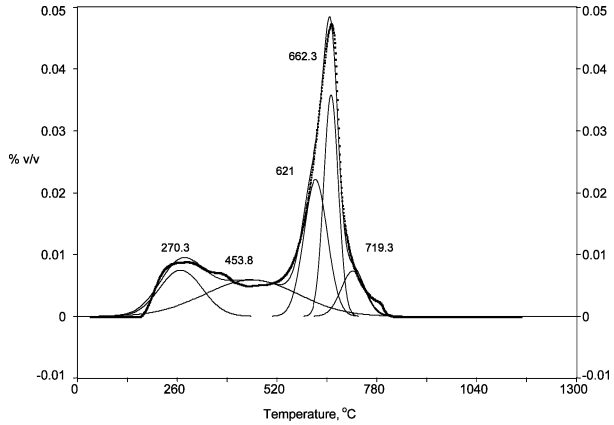

Figure 14. Deconvolution of the CO_2 evolution curve of the RWE activated carbon.

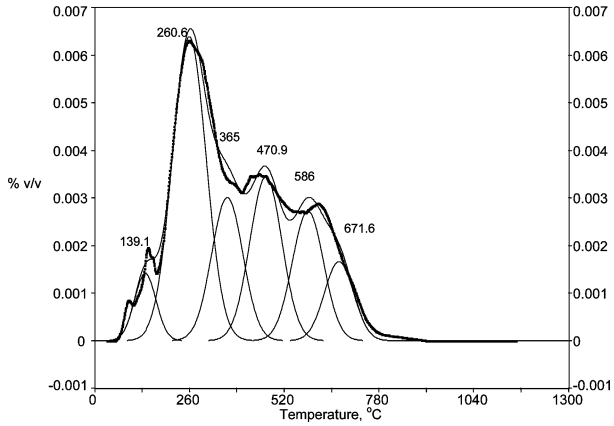

Figure 15. Deconvolution of the CO_2 evolution curve of the F400 activated carbon.

Table 3. Total Gas Evolution during TPD Experiments

	sample	
product gas (mmol/100 g)	RWE	F400
CO	20.9	31.0
CO_2	15.0	4.5
CO/CO_2	1.39	6.89

F440, the basicity is higher than its acidity, which is also confirmed by their measured pH values (Table 4). Thus, basic groups are 15−20% more common than the acidic ones and dominate the surface of both activated carbons. Small differences (∼5%) were observed in the

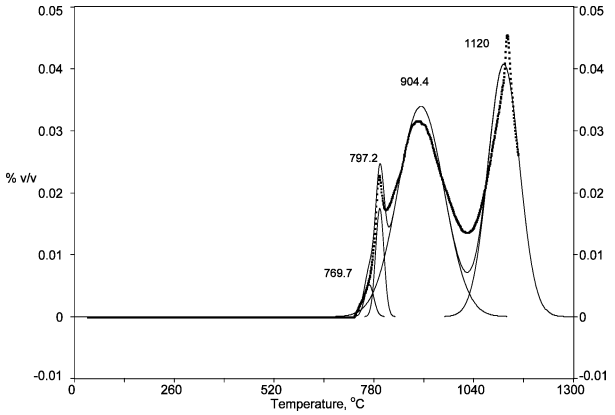

Figure 16. Deconvolution of the CO evolution curve of the RWE activated carbon.

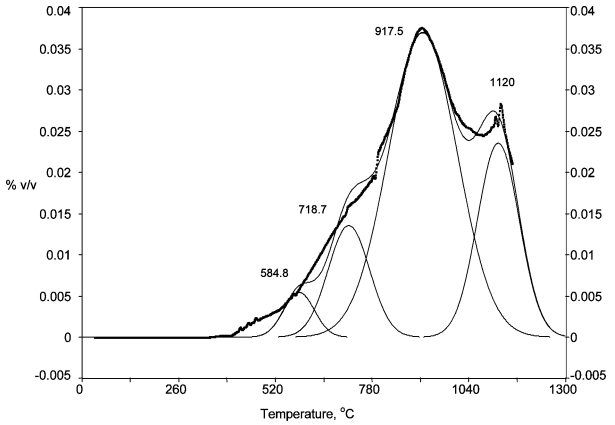

Figure 17. Deconvolution of the CO evolution curve of the F400 activated carbon.

Table 4. Base−Acid Titration Results for the Activated Carbons Tested

	sample	
compound (mmol/100 g)	RWE	F400
$NaHCO_3$	1.7	0.5
Na_2CO_3	7.0	9.4
NaOH	10.0	10.6
HCl	12.3	11.7
pH	10.8	9.0

Table 5. Surface Acidic and Basic Groups of the Activated Carbons Tested

	sample	
functional group (mmol/100 g)	RWE	F400
carboxyls	1.7	0.5
lactones	5.3	8.9
phenols	3.1	1.2
acidic groups	10.1	10.6
basic groups	12.3	11.7
all groups	22.4	22.3

amounts of basic and acid groups between the activated carbons tested. Thus, RWE has more basic groups than F400, while the opposite was observed for the acidic ones. Although both activated carbons exhibited similar amounts of total acidic groups, there are significant differences in the relative amounts of the various oxygen groups (i.e., lactones, phenols, etc.) that constitute the acidic ones (Table 5). RWE has about three times more carboxylic and phenolic groups than F400, while the latter has ~70% more lactonic ones. In both samples, the lactones prevail among the acidic groups. That is particularly true for F400 to which lactonic groups account for ~85% of the total acidic ones. Lactones are much stronger acids than phenols and are quite important, because they are considered as potential active sites for Hg adsorption.[29]

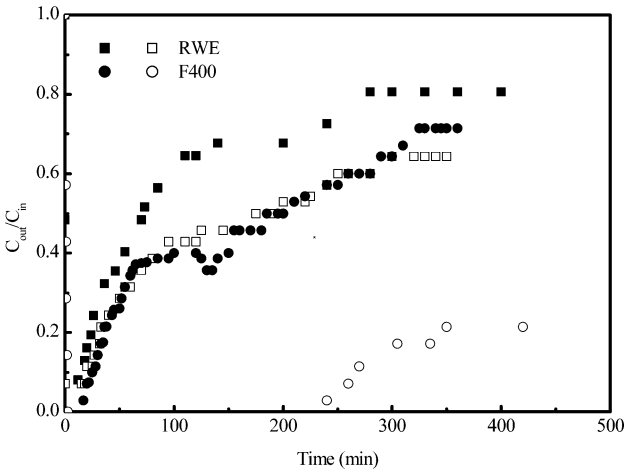

Figure 18. Breakthrough curves of RWE and F400 activated carbons at 50 °C (closed points: raw; open points: sulfur impregnated).

On the basis of the TPD and Boehm titration results, it can be concluded that among the bi-oxygen functional groups carboxyls dominate on the surface of RWE and lactones on the surface of F400. Thus, the observed CO_2 evolution is attributed to the deconvolution of carboxyls for RWE and of lactones for F400.

3.2. Bench-Scale Mercury Adsorption Tests. The Hg° breakthrough curves for raw and sulfur impregnated activated carbons, obtained at 50 °C, are given in Figure 18, and the results on total Hg° removal are summarized in Table 2. The Hg° adsorption capacity of the RWE was found to be much lower than the one of F400 for both raw and sulfur impregnated samples. Adsorption processes are highly affected by the pore structure of the activated carbons. Thus, the high BET surface area and the large pore volume of the microporous F400 enhance Hg° retention, from the gas phase, due to the lower internal mass transfer limitations. Furthermore, the microporous structure of F400 (>80% micropores) further improves its adsorptive capacity, since inside the micropores, where the mechanism of adsorption is pore filling rather than surface coverage, the interaction potential between the solid and the Hg° molecules is significantly higher than that in wider pores.[57] On the other hand, RWE presented lower Hg° adsorptive capacity, as its mesoporous structure enables the penetration of mercury molecules inside the pores and facilitates the faster filling of the limited number of micropores and, thus, the quick saturation of the sample. Therefore, in all temperatures tested, breakthrough curves obtained for RWE were much faster than those obtained for F400, and thus for RWE the outlet concentration reaches the inlet one faster (Figures 19 and 20). Thus, RWE active coke is more suitable for

(57) Carrott, P. J. M.; Roberts, R. A.; Sing, K. S. W. *Characterisation of Porous Solids*; Elsevier: Amsterdam, 1994.

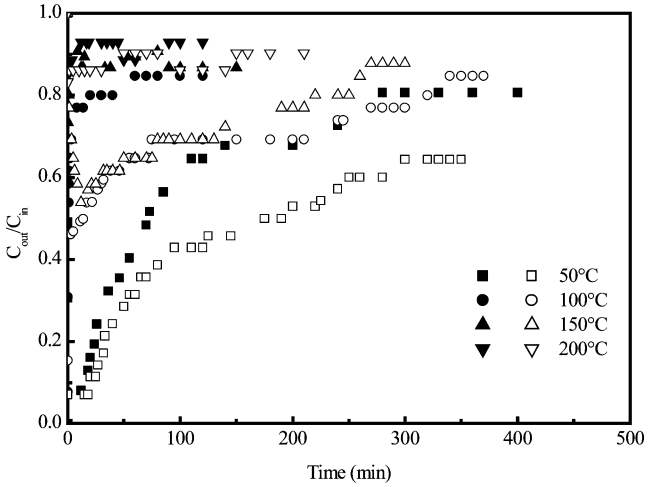

Figure 19. Hg° breakthrough curves for RWE activated carbon at various temperatures (closed points: raw; open points: sulfur impregnated).

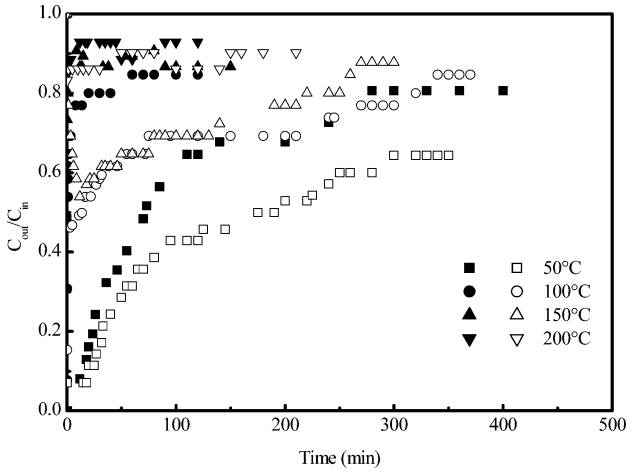

Figure 20. Hg° breakthrough curves for F400 activated carbon at various temperatures (closed points: raw; open points: sulfur impregnated).

continuous Hg removal (i.e., activated carbon injection, low contact time), while Calgon F400 for batch one (i.e., packed column, prolonged contact time).

Apart from pore structure, the surface chemistry and more specifically the surface oxygen functional groups seem to affect the Hg° adsorptive capacity of the activated carbons.[14,29] This was anticipated since an oxidation−reduction mechanism is possibly involved in Hg° adsorption and carbon surface accepts electrons, acting as an electrode.[29,58,59] F400, which displayed higher Hg° retention than RWE, possesses a much larger number of lactonic groups (~70% more) and three times fewer phenolic ones (Table 5). Lactones are stronger acids than phenols and are believed to act as potential active sites for Hg° adsorption[27,29] by participating in the electron-transfer process.[58] In contrast, phenols may inhibit mercury adsorption by reducing the potential of the stabilized structures of carbon surface (electrode), resulting in a lower potential difference that is necessary for the oxidation−reduction reaction involved in Hg° adsorption.[29] Therefore, the enhanced Hg° adsorptive capacity of the F400 activated carbon, apart from its microporous structure, is further justified by the increased number of lactonic groups and the limited presence of phenolic ones on its surface. Thus, F400 acts more effectively as an electrode for electron transfer in Hg°.

In the presence of sulfur, both activated carbons displayed significantly increased mercury adsorption capacity (Figures 19 and 20) that for 50 °C reached about 70% (Table 2). As mentioned previously, the addition of sulfur resulted in limited decrease in N_2 and CO_2 adsorption capacity of F400 and RWE (Figures 4 and 5). Thus, the enhanced Hg° adsorption is attributed to the presence of sulfur since it is very probable that chemisorption, facilitated by HgS formation[7] on the surface area of the activated carbons, controls the ability of the S-impregnated sorbents. In this case, sulfur spread on the carbon surface accepts electrons from mercury and enhances the electrode behavior of the carbon surface.[27,29] The effect of sulfur addition to the microporous F400 (Figure 20) that possesses high BET surface area is more intense, possibly due to the physisorption and chemisorption taking place simultaneously. Thus, when sulfur impregnated F400 is used, 240 min breakthrough time is required to observe mercury in the outlet. Reflecting the above, breakthrough curves became slower for F400 and RWE (Figures 19 and 20). After 360 min, the Hg° outlet concentration reached 20% of the inlet one for F400 and 60% for RWE. The corresponding values for the same time interval are 70 and 80% for F400 and RWE, respectively. Hg° adsorption kinetics, with the presence of sulfur, still remain faster for RWE activated carbon.

When adsorption temperature increases, reduced mercury uptake is observed for both raw and sulfur impregnated F400 and RWE activated carbons (Figures 19 and 20), the reduction being more intense at 150 and 200 °C. Faster breakthrough curves were obtained for all samples, and the outlet concentration approached the inlet one more rapidly. Due to the strong temperature effect, at 200 °C differences in Hg° adsorption capacity between F400 and RWE are diminished. In raw samples, Hg° adsorption is associated with a physisorption mechanism that is a low-temperature process, analogous to condensation,[9,60] and at higher temperatures the mercury adsorption capacity of the activated carbons is reduced. When sulfur is added, the chemisorption mechanism, which comprises the exothermal mercury−sulfur reaction, prevails. The reduction of Hg° held up at higher temperatures is attributed to the exothermal nature of the S−Hg reaction that is advanced by low temperatures[61] and the possible blockage of carbon pores at temperatures above sulfur melting point (115.2 °C). Along this line, for (S) F400 temperature effect becomes significant at adsorption temperatures above 100 °C (Figure 20).

A simple first-order kinetic equation (eq 1) was elaborated to calculate the specific mercury adsorption

(58) Leon, Y.; Leon, C. A.; Radovic, L. R. *Chemistry and Physics of Carbon*; Thrower, P. A., Ed.; Marcel Dekker: New York, 1994; p 213.
(59) Dunham, G. E.; Miller, S. J.; Chang, R.; Bergman, P. *Environ. Prog.* **1998**, *17*, 203−208.
(60) Kwon, S.; Borguet, E.; Vidic, D. R. *Environ. Sci. Technol*. **2002**, *36*, 4162−4169.
(61) Vidic, R.; Siler, D. *Carbon* **2001**, *39*, 3−24.

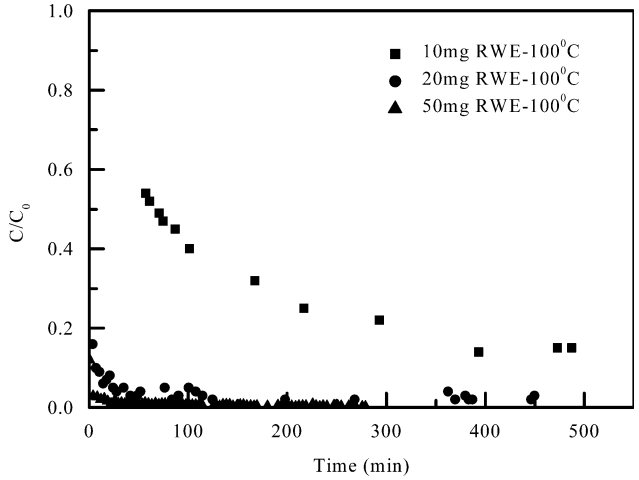

Figure 21. PCB breakthrough curves for RWE activated carbon at 100 °C.

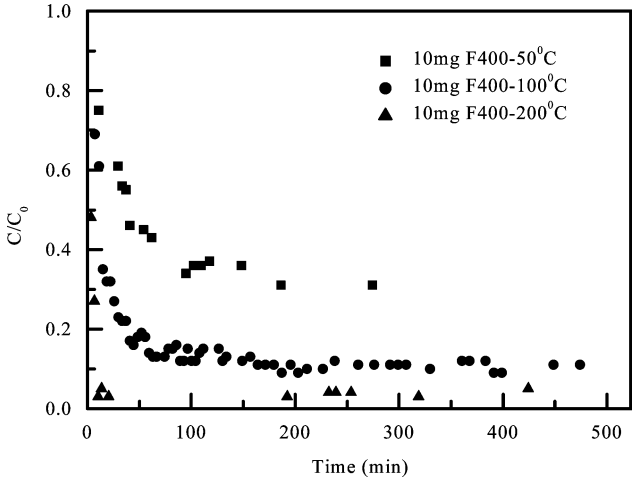

Figure 22. PCB breakthrough curves for F400 activated carbon at various temperatures.

Table 6. Kinetic Parameters of Mercury Adsorption in Raw and Sulfur Impregnated Activated Carbons

			specific adsorption rate (min^{-1})			
sorbent	k_0 (min^{-1})	E (kJ/mol)	50 °C	100 °C	150 °C	200 °C
RWE	17967	36.04	0.0096	0.717	1.18	0.63
(S)RWE	243.44	26.25	0.00625	0.147	0.29	0.11
F400	22292	40.93	0.0037	0.09	0.145	0.609
(S)F400	92.019	34.21	0.00051	0.00055	0.0043	0.028

rates (k_{ads}, min^{-1}) of Hg in the activated carbons, in the linear zone of the breakthrough curves, and the obtained results are given in Table 6.

$$r_{ads} = \frac{d\left(1 - \frac{c_{out}}{c_{in}}\right)}{dt} = k_{ads}\left(1 - \frac{c_{out}}{c_{in}}\right) \Rightarrow$$

$$\ln|1 - \frac{c_{out}}{c_{in}}| = -k_{ads}t \quad (1)$$

Reflecting its faster breakthrough curve the specific Hg° adsorption rate, k_{ads}, for RWE is almost three times higher than the one for F400. At higher temperatures specific adsorption rate increases, the activated carbons are saturated faster, and thus, the mercury outlet concentration reaches the inlet one in shorter time. Indicating the increased mercury adsorption capacity, the presence of sulfur reduces the specific adsorption rate (k_{ads}) for both samples; however, its effect is more intense than that of the microporous F400 activated carbon.

3.3. Bench-Scale PCB Adsorption Tests. The PCB breakthrough curves for RWE and F400 are given in Figures 21 and 22, respectively. Both activated carbons exhibited quite high PCB removal efficiency, and the PCB outlet concentration was very low (almost zero) at 200 °C even after 500 min of testing. Prolongation of adsorption time was meaningless, since the outlet concentration of Hg° reaches the inlet one in much less time. Furthermore, adsorption temperature and activated carbon dosage slightly affect the PCB removal efficiency of both RWE and F400.

3.4. Pilot-Scale Adsorption Tests. Co-combustion tests were carried out using lignite waste blends, and the fuel test matrix is given in Table 7. Aiming to obtain more reliable results, the PCDD/F formation tendency

Table 7. Fuel Blends for Pilot-Scale Trials

code	fuel blend	flue gas flow (Nm^3//hr)
A	lignite/PVC − 97:3	882
B	lignite/sawdust/PVC − 78:19:3	763
C	lignite/sawdust/urea/PVC − 69.8:17.5:10:2.7	958
D	lignite/sawdust/sludge/PVC − 69.8:17.5:10:2.7	845

and the Hg° volatilization potential were enhanced by externally added Cl, thus 3% w/w industrial grade PVC was added in the fuel blends. The obtained results for total Hg and PCDD/F emissions are given in Table 8. When the flue gases pass through the packed column, Hg and PCDD/F emissions are reduced by retention in the activated carbons. Both activated carbons tested were found suitable for mercury and PCDD/F removal from the flue gases, and, in all cases, high removal efficiencies were obtained (Figure 23). Since Hg adsorption is based on physisorption, the microporous F400 shows a bit better performance when used in packed column (prolonged contact time), due to its higher BET surface area, pore volume (mainly micropores), and increased lactone concentration. The addition of sulfur in the activated carbons enhanced further the efficiency of both activated carbons tested, and emissions are reduced down to the detection limit, since chemisorption prevails in this case. This is particularly true for the microporous F400. Quite high (>79%) and in some cases almost complete (>98.5%) PCDD/F removal efficiencies were observed (Figure 23). Thus, as shown in the bench-scale tests, the removal of PCDD/Fs from the gas phase seems not to be a problem for the activated carbons tested, regardless of their pore structure or surface chemistry.

4. Conclusions

Aiming to achieve cleaner combustion of solid fuels, the efficiency in removing toxic polluting compounds (Hg°, PCB, PCDD/F) of two commercial activated carbons (Calgon F400, RWE active coke) was evaluated. The obtained results showed that both activated carbons tested are suitable for the removal of toxic compounds (i.e., Hg, PCBs, PCDD/Fs) from the gas phase. The high BET surface area and large pore volume (mainly micropores) of the microporous F400 enhance Hg° retention

Table 8. Mercury and PCDD/F Measurements during the Pilot-Scale Trials

		inlet concentration[a] (μg/Nm^3)		outlet concentration[a] (μg/Nm^3)		adsorption efficiency (%)	
sorbent	fuel blend	Hg	PCDD/F	Hg	PCDD/F	Hg	PCDD/F
RWE	A	75	0.065	50.3	0.013	33.0	78.7
(S)RWE	D	179	0.070	35.8	0.001	80.0	98.6
F400	B	98	0.044	24.5	0.0084	75.0	81.1
(S)F400	C	126	0.050	9.5	0.00046	92.5	99.1

[a] Isokinetic sampling.

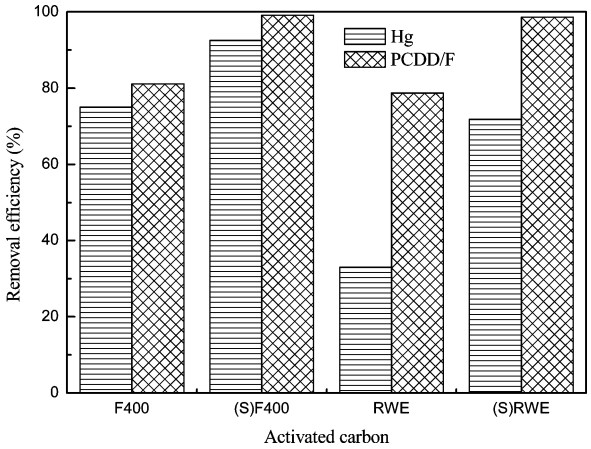

Figure 23. Hg and PCDD/F removal efficiency of the activated carbon tested during pilot-scale tests.

from the gas phase, since inside the micropores, where the mechanism of adsorption is rather pore filling than surface coverage, the interaction potential between the solid and the Hg° molecules is significantly higher than that in wider pores. RWE presented lower Hg° adsorptive capacity, as its mesoporous structure enables the penetration of mercury molecules inside the pores and facilitates the faster filling of the limited number of micropores and, thus, the quick saturation of the sample. Apart from pore structure, the surface chemistry and more specifically the surface oxygen functional groups seem to affect the Hg° adsorptive capacity of the activated carbons, since an oxidation−reduction mechanism is possibly involved in Hg° adsorption and carbon surface accepts electrons, acting as an electrode. Lactones are believed to act as potential active sites for mercury adsorption, while phenols may act as inhibitors. Therefore, the enhanced Hg° adsorptive capacity of the F400 activated carbon could also be attributed to the increased number of lactonic groups and the limited presence of phenolic ones on its surface. Thus, F400 acts more effectively as an electrode for electron transfer from Hg°. In the presence of sulfur, both activated carbons displayed significantly increased mercury adsorption capacity, since chemisorption, facilitated by HgS formation on the surface area of the activated carbons, controls the ability of the S impregnated sorbents. In this case, sulfur spread on the carbon surface accepts electrons from mercury and enhances the electrode behavior of the carbon surface. The effect of sulfur addition to the microporous F400 is more intense, possibly due to the physisorption and chemisorption that take place simultaneously. The Hg adsorption capacity of both raw and sulfur impregnated activated carbons was reduced with temperature increase, because physisorption mechanism is a low-temperature process analogous to condensation, and mercury−sulfur reaction chemisorption is exothermic. The removal of PCBs and PCDD/Fs from the gas phase seems not to be a problem for the activated carbons tested, regardless of their pore structure or surface chemistry.

Acknowledgment. We thank the European Commission for the financial support of this work under Contract No. ECSC 7220-PR/067.

EF050112H